Journal of Public Health and Environmental Research, 2(2):34–43, July-December: 2026.
DOI: https://doi.org/10.58612/jpher224

Journal of Public Health and Environmental Research
ISSN (Online): 3108-3196

Journal homepage: https://www.fpub.org/journal-details.php?journal-id=41

Research Article

Demographic and Spatial Factors Associated with Tuberculosis and Tuberculosis/Human Immunodeficiency Virus Co-infection in Rivers State, Nigeria

Olubunmi D Ihekwaba [1*], Anthony Ike Wegbom [1] and Clement Kevin Edet [2]

[1] *Department of Public Health, Rivers State University, Port Harcourt, Rivers State, Nigeria.*
[2] *Department of Community Medicine, College of Medical Sciences, Rivers State University, Port Harcourt, Rivers State, Nigeria.*
[*] *Corresponding author: olubunmi.ihekwaba@rsu.edu.ng*

Article Info

Keywords: *Tuberculosis, TB/HIV co-infection, Spatial clustering, LISA, Rivers State, Nigeria, Negative binomial regression.*

Received: *02.08.2026;*
Accepted: *11.09.2026;*
Published: *18.09.2026*

Abstract

Background: Tuberculosis (TB) and TB/HIV co-infection remain major public health challenges in Nigeria, but sub-national determinants and statistically confirmed cluster patterns remain poorly characterised. **Objective:** To model demographic and spatial factors associated with TB and TB/HIV co-infection case counts, and to identify annual spatial clusters in Rivers State, Nigeria (2019-2024). **Methods:** Local Government Area (LGA)-level surveillance data were analysed using negative binomial regression with a log-population offset. Spatial autocorrelation and year-specific clustering were assessed using Global Moran's I and Local Indicators of Spatial Association (LISA). **Results:** Of 87,356 TB and 6,643 TB/HIV cases notified, notification rates peaked among working-age adults (25-44 years: adjusted incidence rate ratio [aIRR] = 2.25 for TB and 17.38 for co-infection), upland topography (aIRR = 1.97 for TB and 4.20 for co-infection), and high-density LGAs (aIRR = 2.72 for TB and 5.04 for co-infection). Global Moran's I was non-significant in all years. Locally, Ahoada West was a persistent Low-Low TB coldspot (2021-2024), while a transient High-High TB/HIV hotspot emerged in the Obio/Akpor, Port Harcourt, and Eleme urban corridor in 2022 only. **Conclusion:** TB and TB/HIV distributions are independently associated with population density, topography, and age, with effects strongly amplified for co-infection. The stable TB coldspot reflects systemic access barriers, while the transient co-infection hotspot is programme-linked, requiring targeted, year-specific spatial interventions.

1. Introduction

Tuberculosis (TB) remains one of the world's leading infectious causes of death, claiming approximately 1.25 million lives annually despite the availability of effective curative treatment for more than six decades [1]. The disease is caused by *Mycobacterium tuberculosis*, a slow-growing intracellular pathogen transmitted through aerosolised droplet nuclei expelled by individuals with active pulmonary disease [2]. Among immunocompetent individuals exposed to infection, approximately 90% maintain latent infection without symptomatic disease, while the remaining 10% progress to active disease across their lifetime [3]. When cell-mediated immunity is compromised, particularly through the CD4+ T-lymphocyte depletion associated with human immunodeficiency virus (HIV) infection, the probability of progression from latent to active TB increases substantially and occurs more rapidly [4]. Since its emergence in the early 1980s, HIV has fundamentally

altered TB epidemiology [5]. HIV infection produces progressive depletion of CD4+ T lymphocytes, the cells governing the cell-mediated immune responses required for containment of M. tuberculosis [6], and as immune suppression advances, the risk of progressing from latent TB infection to active disease increases markedly. Epidemiological evidence consistently demonstrates that people living with HIV experience TB risk 15 to 21 times higher than HIV-negative individuals, and TB remains the leading cause of death among people living with HIV, accounting for approximately one-third of acquired immunodeficiency syndrome (AIDS)-related mortality globally [1, 7].

The concurrent circulation of TB and HIV within populations produces a syndemic, a form of disease interaction in which biological reinforcement combines with social concentration to intensify population-level burden beyond what would be expected if the two infections operated independently [8]. This interaction is characterised by reciprocal biological mechanisms wherein HIV-related immune suppression facilitates TB acquisition and progression, while active TB induces pro-inflammatory states that promote HIV replication and accelerate immune decline [9]. Sub-Saharan Africa carries the heaviest weight of this syndemic globally, accounting for approximately 23% of global TB cases yet more than 70% of TB cases occurring among people living with HIV [1].

Within sub-Saharan Africa, Nigeria occupies a critical position in the global TB and co-infection dilemma, ranking among the top three high-burden TB countries globally and carrying one of the highest TB/HIV co-infection burdens in the world [1]. National estimates indicate that approximately 25.8% of TB cases in Nigeria occur among people living with HIV [10]. The Niger Delta region of Nigeria, characterised by sustained petroleum extraction, rapid urbanisation, and environmental degradation, presents particularly complex epidemiological conditions: labour migration linked to petroleum employment produces transient working populations whose social networks span multiple geographic areas and whose housing is frequently informal and crowded, while terrain varies from dense urban centres to isolated wetland and riverine communities, creating extreme heterogeneity in distance to healthcare facilities and accessibility of diagnostic services.

National-level estimates nevertheless conceal substantial sub-national variation, as TB case detection rates, HIV prevalence estimates, health system capacity, and patterns of healthcare accessibility all vary considerably between states [11, 12]. Studies documenting TB and co-infection in Rivers State exist at facility level [13], and prior spatial-temporal analysis has identified persistently elevated TB burden in urban Local Government Areas (LGAs) [14]; however, no study has identified which demographic and spatial characteristics of an LGA are independently associated with notification burden, nor formally tested whether that burden exhibits statistically significant geographic clustering, or distinguished genuinely persistent spatial concentrations from the transient programme effects documented for targeted outreach and hotspot-directed case-finding elsewhere in Nigeria [15, 16]. None has applied formal cluster statistics on a year-by-year basis, the approach required to distinguish persistent spatial structure from transient clustering, and none has examined the period 2019-2024, which spans pre-pandemic baseline conditions, the acute disruption phase of the coronavirus disease 2019 (COVID-19) pandemic, and the subsequent period of health system adaptation [17].

The consequence of this evidence void falls on programme managers in Rivers State, who are responsible for TB and HIV control under persistent fiscal, infrastructural, and workforce constraints, and for whom effective planning depends on evidence that extends beyond aggregated state-level indicators. Generating granular information on where disease burden is concentrated within the state, which LGAs merit intensified intervention, which demographic groups carry the highest risk, and whether pandemic disruption affected different areas differently would enable informed prioritisation. The requirement is therefore for longitudinal, spatially disaggregated analysis of TB and co-infection notifications across Rivers State's 23 LGAs between 2019 and 2024, employing formal spatial-temporal analytical methods capable of identifying geographic clustering and distinguishing detection-driven from transmission-driven notification increases. Such analysis would address a critical gap in the Nigerian TB/HIV evidence base and would provide Rivers State programmes with an empirical foundation for geographically targeted, demographically informed resource allocation.

This study therefore examined two questions: first, which demographic and spatial characteristics of an LGA are independently associated with TB and TB/HIV co-infection case counts once other covariates are held constant; and second, whether TB and TB/HIV notification rates across the 23 LGAs exhibit statistically significant spatial clustering and, if so, whether such clustering is geographically stable or transient across the six-year period from 2019 to 2024.

2. Methods

2.1. Study Setting and Design

An ecological design was used, analysing aggregated data at LGA level rather than individual-level data [18], consistent with Nigeria's TB surveillance system, which reports notifications by administrative boundary. The study covered all 23 LGAs of Rivers State over 2019-2024, a window spanning pre-pandemic conditions, acute COVID-19 disruption, and post-pandemic adaptation. Rivers State lies in the Niger Delta region of southern Nigeria (4°15'-5°45'N, 5°22'-7°35'E) and comprises 23 LGAs. Port Harcourt, the state capital, hosts the headquarters of major petroleum companies and attracts substantial labour migration. The geography is heterogeneous: upland LGAs with stable terrain and road access contrast with riverine LGAs of creeks and island communities accessible primarily by boat; metropolitan LGAs such as Port Harcourt City and Obio/Akpor are densely populated and well served by health infrastructure, whereas rural LGAs have dispersed settlements and limited diagnostic access. HIV prevalence is approximately 3.8%, above the national average of 1.3-1.4% [19, 20].

2.2. Data Sources and Variable Construction

Annual TB and TB/HIV case counts, disaggregated by LGA, age group, and sex, were obtained for 2019-2024 from the Rivers State Tuberculosis, Leprosy and Buruli Ulcer Control Programme (State Ministry of Health), which compiles notifications from facilities in all 23 LGAs under the National Tuberculosis and Leprosy Control Programme framework.

Population density was calculated by dividing National Population Commission projected population figures, based on the 2006 census, by LGA land area (persons/km²), and categorised into low, medium, and high tertiles. Rivers State LGAs were classified geographically as riverine or upland using data from the Ministry of Physical Planning, the National Bureau of Statistics, and geographic studies, while urban-rural statuses were determined via the Degree of Urbanisation framework, designating Port Harcourt City, Obio-Akpor, Eleme, Oyigbo, Okrika, Ikwerre, and Bonny as urban or peri-urban due to metropolitan integration and industrial development.

LGA boundary data (Admin Level 2) were obtained from the Humanitarian Data Exchange (OCHA) and processed in Python using

GeoPandas; LGA names were standardised and joined to the case data at LGA level.

2.3. Study Outcomes and Predictors

Outcomes were the TB and TB/HIV case counts notified per LGA over 2019-2024. Predictors were age group (0-15, 16-24, 25-44, 45-64, $\geq$ 65 years), sex (female, male), settlement type (rural, urban), topography (riverine, upland), and population density (low, medium, high). The log-transformed LGA population entered all models as an exposure offset to account for variation in LGA population size.

2.4. Statistical Analysis and Model Selection

Overdispersion was assessed by comparing each outcome's variance with its mean; a variance-to-mean ratio exceeding 1 favours negative binomial over Poisson regression Table 1. Both outcomes were modelled as generalised linear models with a log-link and the log-population offset. Bivariate (unadjusted) models were fitted for each predictor, followed by a multivariate model including all predictors simultaneously, to identify confounding. Coefficients were exponentiated as incidence rate ratios (IRR = e^{β}); significance was set at $p < 0.05$.

Cluster detection was performed separately for each year rather than on pooled six-year totals, to capture cluster formation and dissolution. Annual notification rates (cases per 100,000 projected population) were tested for global spatial autocorrelation (Global Moran's I), followed by Local Moran's I (LISA) using the esda library with queen contiguity weights (libpysal) in Python. Each LGA was classified as High-High, Low-Low, High-Low, or Low-High relative to its neighbours; significance was assessed by conditional permutation at $p < 0.05$.

2.5. Ethical Considerations

Ethical approval was obtained from the Rivers State Ministry of Health and Hospital Management Board and from the Research Ethics Committee, Faculty of Basic Medical Sciences, Rivers State University. The data were pre-aggregated, de-identified LGA totals without patient-level identifiers, so individual consent was not applicable. Authorised access was granted through approval letters and written introduction.

3. Results

3.1. Model Selection and Overdispersion Diagnostics

The mean cumulative TB case count across the 23 LGAs was 3,798.09, against a variance of 12,391,890.63, generating a dispersion ratio of 3,262.66. For TB/HIV co-infection, the mean was 288.83 against a variance of 203,472.97, generating a dispersion ratio of 704.47. Both dispersion ratios substantially exceeded the threshold of 1, confirming significant overdispersion in both outcomes and supporting the selection of negative binomial regression for subsequent modelling Table 1.

Table 1: Model diagnostic and overdispersion analysis for count data selection

Variable	Mean (μ)	Variance (σ^2)	Dispersion ratio (ϕ)	Interpretation
Total TB cases (n = 23 LGAs)	3,798.09	12,391,890.63	3,262.66	Significant overdispersion
Total TB/HIV co-infection cases (n = 23 LGAs)	288.83	203,472.97	704.47	Significant overdispersion

3.2. Demographic and Spatial Characteristics of Reported Cases

Over the six-year period 2019-2024, a cumulative 87,356 TB cases and 6,643 TB/HIV co-infection cases were recorded across the 23 LGAs. The 25-44 years age category accounted for the largest share of both TB cases (34.6%, n = 30,187) and co-infection cases (50.5%, n = 3,358). The 45-64 years age group recorded 25.4% of TB cases (n = 22,156) and 28.5% of co-infection cases (n = 1,894). The 16-24 years age group accounted for 16.3% of TB cases (n = 14,233) and 12.5% of co-infection cases (n = 827). The 0-15 years age group recorded 16.0% of TB cases (n = 13,969) and 4.5% of co-infection cases (n = 301). The 65 years and above age group accounted for 7.8% of TB cases (n = 6,811) and 4.0% of co-infection cases (n = 263).

Males accounted for 51.5% of TB cases (n = 45,027) and 52.2% of co-infection cases (n = 3,467); females accounted for 48.5% of TB cases (n = 42,329) and 47.8% of co-infection cases (n = 3,176). The male-to-female ratio was 1.06:1 for TB and 1.09:1 for co-infection.

Urban/Peri-Urban LGAs accounted for 38.9% of TB cases (n = 33,995) and 62.3% of co-infection cases (n = 4,140), while rural LGAs contributed 61.1% of TB cases (n =53,401) and 37.7% of co-infection cases (n = 2,503). Upland LGAs recorded 79.1% of TB cases (n = 69,091) and 93.7% of co-infection cases (n = 6,226), while riverine LGAs accounted for 20.9% of TB cases (n = 18,265) and 6.3% of co-infection cases (n = 417). Medium-density LGAs recorded the largest share of TB cases (42.4%, n = 37,038), while high-density LGAs accounted for the largest share of co-infection cases (63.4%, n = 4,213). Low-density LGAs accounted for 19.1% of TB cases (n = 16,655) and 7.8% of co-infection cases (n = 519) Table 2.

Table 2: Demographic and spatial characteristics of TB and TB/HIV co-infection distribution in Rivers State (2019-2024)

Predictor covariate	TB cases (n = 87,356)	TB/HIV co-infection cases (n = 6,643)
Age group (years)		
0-15	13,969 (16.0%)	301 (4.5%)
16-24	14,233 (16.3%)	827 (12.5%)
25-44	30,187 (34.6%)	3,358 (50.5%)
45-64	22,156 (25.4%)	1,894 (28.5%)
65+	6,811 (7.8%)	263 (4.0%)
Biological sex		
Female	42,329 (48.5%)	3,176 (47.8%)
Male	45,027 (51.5%)	3,467 (52.2%)
Geographic setting		
Rural LGAs	53,401 (61.1%)	2,503 (37.7%)
Urban LGAs	33,955 (38.9%)	4,140 (62.3%)
Topographical layout		
Riverine LGAs	18,265 (20.9%)	417 (6.3%)
Upland LGAs	69,091 (79.1%)	6,226 (93.7%)
Population density category		
Low	16,655 (19.1%)	519 (7.8%)
Medium	37,038 (42.4%)	1,911 (28.8%)
High	33,663 (38.5%)	4,213 (63.4%)

3.3. Demographic and Spatial Factors Associated with TB Cases

In the bivariate analysis, TB notification rate was significantly elevated in the 25-44 years age group compared to children aged 0-15 years (crude IRR = 2.126, 95% CI: 1.538-2.938, $p < 0.001$) and in the 45-64 years age group (crude IRR = 1.421, 95% CI: 1.028-1.964, p = 0.033). The 16-24 years age group showed a lower but non-significant association (crude IRR = 0.782, 95% CI: 0.566-1.081, p = 0.137). The 65 years and above age group showed a significantly lower notification rate compared to children aged 0-15 years (crude IRR = 0.271, 95% CI: 0.196-0.375, $p < 0.001$). Male sex was not significantly associated with TB notification rate (crude IRR = 1.062, 95% CI: 0.820-1.376, p = 0.648). Urban residence showed a non-significant association in the unadjusted analysis (crude IRR = 0.884, 95% CI: 0.667-1.171, p = 0.389). Upland topography was significantly associated with higher notification rate (crude IRR = 1.952, 95% CI: 1.497-2.546, $p < 0.001$). Medium-density LGAs showed a significantly lower notification rate relative to low-density LGAs (crude IRR = 0.545, 95% CI: 0.415-0.715, $p < 0.001$), while high-density LGAs showed a significantly higher notification rate (crude IRR = 2.774, 95% CI: 2.114-3.640, $p < 0.001$).

After adjustment for all covariates simultaneously, the 25-44 years age group remained significantly associated with higher TB notification rate (adjusted IRR = 2.253, 95% CI: 1.496-3.394, $p < 0.001$), as did the 45-64 years age group (adjusted IRR = 1.610, 95% CI: 1.069-2.425, p = 0.023). The 65 years and above age group remained significantly lower (adjusted IRR = 0.365, 95% CI: 0.242-0.551, $p < 0.001$). The 16-24 years age group remained non-significant after adjustment (adjusted IRR = 1.019, 95% CI: 0.676-1.536, p = 0.928), with the direction of the association shifting from negative to positive relative to the crude estimate. Male sex remained non-significant (adjusted IRR = 1.090, 95% CI: 0.841-1.413, p = 0.514). Urban setting became significantly associated with higher notification rate only after adjustment (adjusted IRR = 1.612, 95% CI: 1.179-2.204, p = 0.003), in contrast to the non-significant unadjusted estimate. Upland topography remained significantly associated with higher notification rate (adjusted IRR = 1.970, 95% CI: 1.472-2.636, $p < 0.001$). Medium-density LGAs remained significantly lower after adjustment (adjusted IRR = 0.517, 95% CI: 0.330-0.811, p = 0.004), while high-density LGAs remained significantly higher (adjusted IRR = 2.715, 95% CI: 1.940-3.799, $p < 0.001$) Table 3.

Table 3: Bivariate and multivariate negative binomial regression analysis of the association between demographic and spatial factors and TB cases

Predictor	Unadjusted IRR (95% CI)	p	Adjusted IRR (95% CI)	p
Age (reference: 0-15 years)				
16-24	0.782 (0.566-1.081)	0.137	1.019 (0.676-1.536)	0.928
25-44	2.126 (1.538-2.938)	<0.001	2.253 (1.496-3.394)	<0.001
45-64	1.421 (1.028-1.964)	0.033	1.610 (1.069-2.425)	0.023
65+	0.271 (0.196-0.375)	<0.001	0.365 (0.242-0.551)	<0.001
Sex (reference: female)				
Male	1.062 (0.820-1.376)	0.648	1.090 (0.841-1.413)	0.514
Geographic setting (reference: rural)				
Urban	0.884 (0.667-1.171)	0.389	1.612 (1.179-2.204)	0.003
Topography (reference: riverine)				
Upland	1.952 (1.497-2.546)	<0.001	1.970 (1.472-2.636)	<0.001
Population density (reference: low)				
Medium	0.545 (0.415-0.715)	<0.001	0.517 (0.330-0.811)	0.004
High	2.774 (2.114-3.640)	<0.001	2.715 (1.940-3.799)	<0.001

3.4. Demographic and Spatial Factors Associated with TB/HIV Co-infection Cases

In the bivariate analysis, the 25-44 years age group carried a substantially elevated crude notification rate of co-infection (crude IRR = 4.144, 95% CI: 2.986-5.752, $p < 0.001$), while the 65 years and above group showed a significantly lower notification rate (crude IRR = 0.142, 95% CI: 0.099-0.203, $p < 0.001$). The 16-24 years age group showed a lower but non-significant association (crude IRR = 0.738, 95% CI: 0.529-1.028, p = 0.073), while the 45-64 years age group showed a borderline association (crude IRR = 1.390, 95% CI: 1.000-1.932, p = 0.050). Male sex was not significantly associated with co-infection in the unadjusted analysis (crude IRR = 1.045, 95% CI: 0.802-1.361, p = 0.746). Urban setting was significantly associated with higher co-infection notification rate (crude IRR = 1.952, 95% CI: 1.466-2.598, $p < 0.001$). Upland topography showed a substantially elevated crude notification rate (crude IRR = 5.514, 95% CI: 4.163-7.302, $p < 0.001$). Both medium-density LGAs (crude IRR = 1.511, 95% CI: 1.145-1.992, p = 0.004) and high-density LGAs (crude IRR = 1.616, 95% CI: 1.224-2.133, $p < 0.001$) showed significantly higher notification rates compared to low-density LGAs.

In the adjusted model, effect sizes were substantially larger than in the bivariate analysis. The 16-24 years age group, non-significant in the bivariate model, was significantly elevated after adjustment (adjusted IRR = 4.181, 95% CI: 2.593-6.739, $p < 0.001$). Relative to children aged 0-15 years, the adjusted notification rate of co-infection was 17.379 times higher among 25-44 year-olds (95% CI: 10.887-27.742, $p < 0.001$) and 8.187 times higher among 45-64 year-olds (95% CI: 5.110-13.118, $p < 0.001$). The 65 years and above age group became non-significant after adjustment (adjusted IRR = 0.796, 95% CI: 0.475-1.334, p = 0.387). Male sex remained non-significant (adjusted IRR = 1.031, 95% CI: 0.772-1.378, p = 0.835). Urban setting remained significantly associated with higher notification rate (adjusted IRR = 2.618, 95% CI: 1.851-3.703, $p < 0.001$). Upland topography remained significant (adjusted IRR = 4.201, 95% CI: 2.993-5.897, $p < 0.001$). Medium-density LGAs became non-significant after adjustment (adjusted IRR = 1.249, 95% CI: 0.747-2.086, p = 0.397), while high-density LGAs remained significant, with a substantially larger adjusted effect size (adjusted IRR = 5.043, 95% CI: 3.449-7.375, $p < 0.001$) Table 4.

Table 4: Bivariate and multivariate negative binomial regression analysis of the association between demographic and spatial factors and TB/HIV co-infection cases

Predictor	Unadjusted IRR (95% CI)	p	Adjusted IRR (95% CI)	p
Age (reference: 0-15 years)				
16-24	0.738 (0.529-1.028)	0.073	4.181 (2.593-6.739)	<0.001
25-44	4.144 (2.986-5.752)	<0.001	17.379 (10.887-27.742)	<0.001
45-64	1.390 (1.000-1.932)	0.050	8.187 (5.110-13.118)	<0.001
65+	0.142 (0.099-0.203)	<0.001	0.796 (0.475-1.334)	0.387
Sex (reference: female)				
Male	1.045 (0.802-1.361)	0.746	1.031 (0.772-1.378)	0.835
Geographic setting (reference: rural)				
Urban	1.952 (1.466-2.598)	<0.001	2.618 (1.851-3.703)	<0.001
Topography (reference: riverine)				
Upland	5.514 (4.163-7.302)	<0.001	4.201 (2.993-5.897)	<0.001
Population density (reference: low)				
Medium	1.511 (1.145-1.992)	0.004	1.249 (0.747-2.086)	0.397
High	1.616 (1.224-2.133)	<0.001	5.043 (3.449-7.375)	<0.001

3.5. Global and Local Spatial Clustering of TB

Global Moran's I for TB notification rates was non-significant in every year of the study period, with p-values exceeding 0.05 in all six years (2019: p = 0.2754; 2020: p = 0.7337; 2021: p = 0.8860; 2022: p = 0.4715; 2023: p = 0.3691; 2024: p = 0.7732), indicating that state-wide TB notification rates did not depart overall from a random spatial arrangement.

At the local level, a persistent Low-Low coldspot pattern emerged in later years. In 2019, Akuku-Toru, a riverine LGA, was identified as a statistically significant High-Low spatial outlier, defined as a high-notification LGA surrounded by low-notification neighbours; this classification did not recur in any subsequent year. No significant local clusters or outliers were detected in 2020. Beginning in 2021, Ahoada West was identified as a statistically significant Low-Low coldspot and remained so in each subsequent year through 2024. No LGA was identified as a statistically significant High-High hotspot for TB in any year Table 5, Figure 1.

Table 5: Year-by-year Global Moran's I significance and local LISA cluster results for TB case notification rates (2019-2024)

Year	Global Moran's I p-value	Significant LISA cluster type ($p < 0.05$)	LGA count	LGA(s) implicated
2019	0.2754	High-Low outlier	1	Akuku-Toru
2020	0.7337	None detected	0	-
2021	0.8860	Low-Low cluster (coldspot)	1	Ahoada West
2022	0.4715	Low-Low cluster (coldspot)	1	Ahoada West
2023	0.3691	Low-Low cluster (coldspot)	1	Ahoada West
2024	0.7732	Low-Low cluster (coldspot)	1	Ahoada West

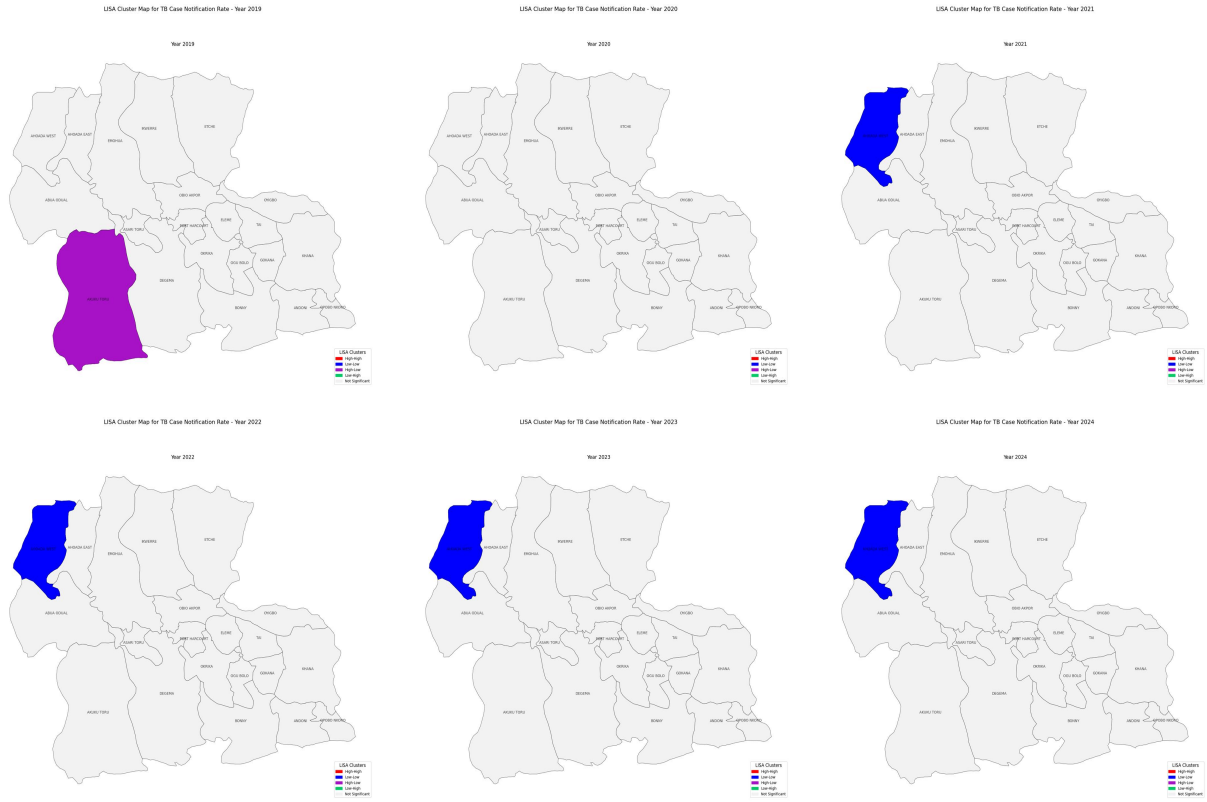

Figure 1: LISA cluster maps of significant local spatial association for TB case notification rates per 100,000 population across the 23 Local Government Areas of Rivers State, (a) 2019 through (f) 2024. Local Moran's I under queen contiguity weights; significance by conditional permutation at $p < 0.05$. High-High = hotspot; Low-Low = coldspot; High-Low/Low-High = spatial outliers; Not Significant includes areas whose local statistic did not reach significance

3.6. Global and Local Spatial Clustering of TB/HIV Co-infection

Global Moran's I for co-infection notification rates was likewise non-significant in every year, including 2022, when local clustering reached its maximum extent (2019: p = 0.8482; 2020: p = 0.6295; 2021: p = 0.6909; 2022: p = 0.2405; 2023: p = 0.9800; 2024: p = 0.9683). No significant local clusters or outliers were detected in 2019 or 2020. In 2021, Oyigbo emerged as a statistically significant Low-Low coldspot. In 2022, local clustering reached its maximum, with three contiguous LGAs (Obio/Akpor, Port Harcourt, and Eleme) identified as statistically significant High-High clusters, while Oyigbo persisted as a Low-Low coldspot. This cluster structure dissolved entirely in 2023, with no LGA registering as significant in any category, and no significant local clustering was detected in 2024 Table 6, Figure 2.

Table 6: Year-by-year Global Moran's I significance and local LISA cluster results for TB/HIV co-infection case notification rates (2019-2024)

Year	Global Moran's I p-value	Significant LISA cluster type ($p < 0.05$)	LGA count	LGA(s) implicated
2019	0.8482	None detected	0	-
2020	0.6295	None detected	0	-
2021	0.6909	Low-Low cluster (coldspot)	1	Oyigbo
2022	0.2405	High-High cluster (hotspot)	3	Obio/Akpor, Port Harcourt, Eleme
2022	0.2405	Low-Low cluster (coldspot)	1	Oyigbo
2023	0.9800	None detected	0	-
2024	0.9683	None detected	0	-

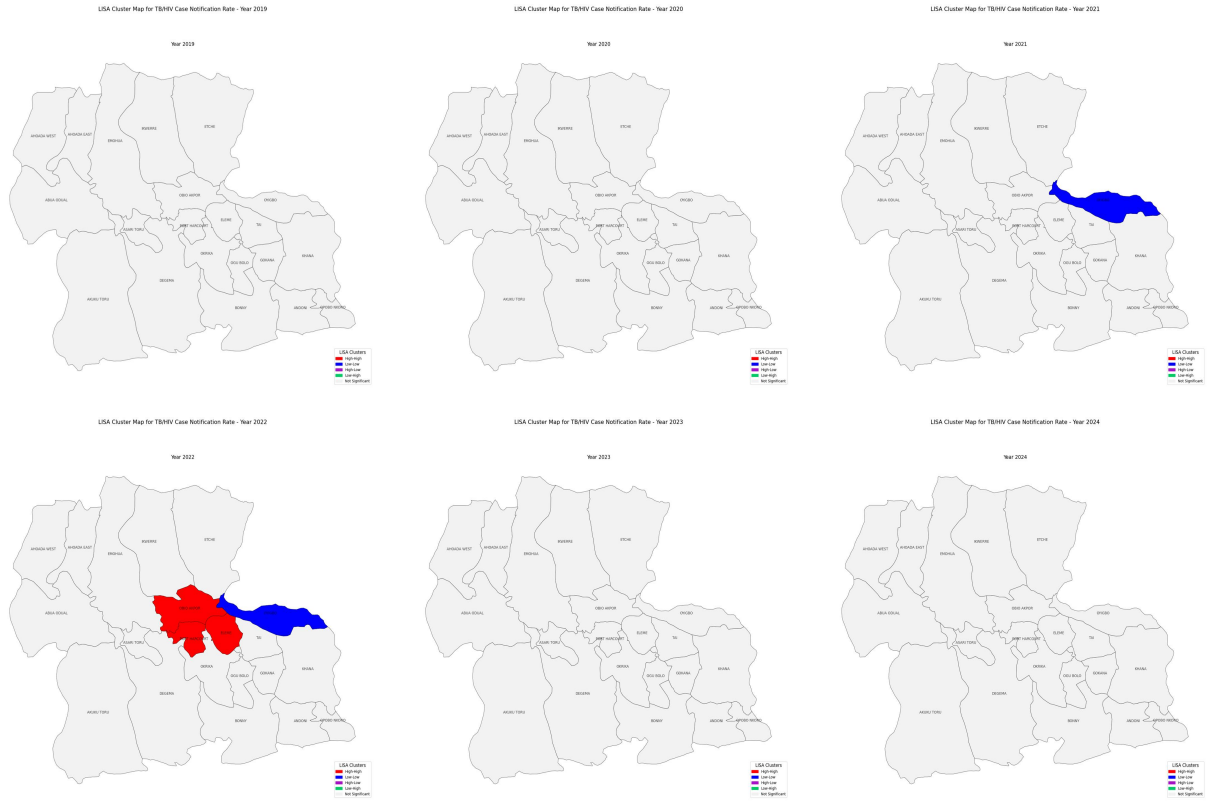

Figure 2: LISA cluster maps of significant local spatial association for TB/HIV co-infection case notification rates per 100,000 population across the 23 Local Government Areas of Rivers State, (a) 2019 through (f) 2024. Local Moran's I under queen contiguity weights; significance by conditional permutation at $p < 0.05$. High-High = hotspot; Low-Low = coldspot; High-Low/Low-High = spatial outliers; Not Significant includes areas whose local statistic did not reach significance

4. Discussion

4.1. Demographic and Spatial Determinants

Of all the predictors examined, age produced the largest effect sizes, with co-infection notification concentrated overwhelmingly in the working-age population and this concentration strengthening after adjustment for geographic covariates Table 4. Facility-based reports from other Nigerian states identify working-age adults as the highest-burden group for TB/HIV co-infection, linked to occupational and sexual-network exposure [21], a pattern consistent with the composition of Rivers State's petroleum-sector and informal-trade employment base. Other Nigerian studies have, however, located the highest co-infection burden in different age groups depending on the population sampled, whether general directly observed treatment, short-course (DOTS) attendees [22], national samples of HIV-positive key populations [23], or treatment-centre presentations [24], indicating that a single national age-risk profile for TB/HIV co-infection should not be assumed independent of the population a given data source captures.

Neither TB nor TB/HIV notification showed a significant association with sex at any stage of the analysis, a null finding that requires interpretation with reference to the ecological design. Because an LGA-level regression detects a sex effect only where the proportion of male and female cases varies systematically across LGAs, a true individual-level sex differential that is approximately constant across all 23 LGAs leaves the model with no cross-LGA variation to detect. The null finding should therefore not be read as evidence against a sex-based risk differential at the individual level, a question for which facility-based clinical studies remain the more appropriate evidence source [24].

Among the spatial predictors, population density carried the largest effect for both outcomes, and its effect on co-infection increased substantially after adjustment Table 4, consistent with dense LGAs concentrating not only TB diagnostic capacity but also HIV testing and antiretroviral therapy services. That medium-density LGAs lost significance after adjustment indicates a co-infection density effect concentrated in the highest-density urban core rather than operating as a smooth gradient across the density spectrum. Upland topography, which remained a significant independent predictor of both outcomes after adjustment, increasing slightly for TB and attenuating for co-infection Tables 3 and 4, behaved as a distinct structural pathway rather than a proxy for settlement type or crowding, since its effect persisted despite control for both, and facility-access gradients reported elsewhere in Nigeria show a comparable pattern [12].

Beyond density and terrain, the urban notification concentration is consistent with referral-driven case attribution documented for drug-resistant TB in Kaduna State, where a majority of recorded patients were urban residents despite likely mixed rural-urban origin [25]; the LGA-resolution data used here cannot distinguish referral effects from genuine urban excess. In the opposite direction, a tertiary-facility study in Enugu State reported lower odds of co-infection among urban residents after adjusting for occupation [26], underscoring that facility catchment and LGA of residence do not necessarily yield the same answer to the same question. For TB specifically, the urban-setting result illustrates a confounding pattern visible in Table 3: the bivariate association between urban residence and notification rate was null but became strongly significant only after adjusting for topography, consistent with substantial overlap between the urban and upland classifications in Rivers State, such that the crude urban effect was masked until topographic confounding was removed. Fundamental

Cause Theory [27] offers one framework for interpreting the persistence of the terrain effect, holding that socioeconomic position, of which geographic isolation is one structural expression, determines access to the flexible resources, including transport, information, and proximity to services, needed to convert symptomatic illness into a diagnosed and notified case. Disease Ecology Theory [28] complements this account by explaining why terrain rather than settlement classification carries the strongest independent effect: the physical and ecological conditions of a place, including how terrain constrains population movement and service reach, shape whether disease is detected as much as whether it is transmitted.

4.2. Spatial Cluster Detection

In contrast to most prior Nigerian applications, which applied cluster statistics to pooled or shorter time periods rather than testing each year for persistence [16, 29], this study applied local spatial statistics separately to each year. The distinction proved analytically consequential: a pooled six-year analysis of this dataset would very likely have identified Port Harcourt and its neighbouring LGAs as a stable co-infection hotspot, given the substantially elevated cumulative case totals recorded there, whereas the year-by-year analysis identified this pattern as a single-year event (2022) confined to TB/HIV co-infection specifically, with no TB hotspot confirmed in any year of the series Tables 5 and 6; Figures 1 and 2. Annual disaggregation therefore distinguished a genuinely persistent structural pattern from a transient, programme-linked one in a way that pooled analysis could not.

Measured against the rest of the TB series, the Ahoada West coldspot stands as the most robust spatial finding of this analysis: a statistically confirmed Low-Low cluster in four of six years Table 5, Figure 1, persisting while the state-wide maximum notification rate increased substantially over the same years. That the detection deficit remained stable while notification intensified elsewhere in the state indicates a structural, place-based barrier to case detection rather than a lag expected to close as diagnostic capacity expanded. Equally notable is the asymmetry at the opposite end of the distribution: no TB High-High hotspot was confirmed in any year, despite pronounced and sustained increases in the state-wide notification maximum, indicating that detection gains concentrated in the urban upland core never achieved sufficient local spatial coherence relative to immediately neighbouring LGAs to register as a statistically confirmed cluster under queen contiguity at LGA resolution, even as a stable low-detection cluster was repeatedly confirmed.

Where the TB coldspot signalled stability, the co-infection pattern signalled episodic activity Table 6, Figure 2. The single-year emergence of a three-LGA High-High cluster in the industrial corridor spanning Obio/Akpor, Port Harcourt, and Eleme, followed by its complete dissolution the following year, alongside a persistent low-detection classification in the immediately adjacent LGA of Oyigbo across the same two years, suggests that the 2022 co-infection surge reflected a geographically confined programmatic effect, plausibly linked to intensified HIV testing activity at specific facilities within this corridor, rather than a systematic, structurally embedded spatial process comparable to the TB coldspot. Ecosocial Theory and the concept of biological embodiment of structural conditions [30] offer a compatible reading: a cluster that appears and disappears within a single year is more readily explained by a bounded period of intensified local service delivery than by a fixed geography of underlying risk.

4.3. Interpretation of Non-Significant Global Statistics

Although Global Moran's I was non-significant for both diseases in every year examined, the 2022 results, in which local LISA statistics identified four significant local classifications for co-infection Table 6, Figure 2, show why this apparent discrepancy is not a contradiction [31]. Global Moran's I tests whether the overall spatial arrangement across all 23 LGAs departs from randomness, while local LISA statistics test each LGA individually against its immediate neighbours; a small number of sharply localised clusters embedded within an otherwise randomly arranged field, as occurred in the 2022 co-infection pattern, can therefore coexist with global non-significance. Reliance on a global statistic alone would have concealed the single most important spatial finding in the co-infection series.

4.4. Limitations

Because the study is ecological in design, every association reported between age, sex, topography, settlement type, or density and case counts describes a relationship between LGA-level characteristics and LGA-level totals, not between individual exposures and individual outcomes; the null sex finding illustrates this limitation directly, as an absence of ecological association does not establish an absence of individual-level risk difference. Surveillance notification data record diagnosed and reported disease rather than incidence directly, so the regression associations reported here capture determinants of notified case counts, which reflect both underlying transmission and diagnostic capacity, and the two cannot be fully separated with the data available. Population figures underlying the density classification trace back to Nigeria's last full enumeration in 2006 rather than a contemporary count; because the same projection method was applied uniformly to all 23 LGAs, any resulting error is likely non-differential, but some misclassification relative to the true 2019-2024 population distribution cannot be ruled out. A further constraint arises from the number of spatial units: the 23 LGAs available for local spatial analysis sit at the lower end of what is recommended for stable local spatial autocorrelation inference [31, 32], a constraint that elevates the risk of Type II error and applies to all non-significant local results reported here, including the absence of a confirmed TB hotspot, which should be read as inconclusive rather than as evidence of a genuinely uniform spatial pattern in the urban core.

5. Conclusion

In Rivers State, TB and TB/HIV co-infection case distribution is independently associated with working-age adult status, upland topography, and high population density, each exerting a substantially larger effect on TB/HIV co-infection than on TB alone. Formal cluster analysis conducted separately for each year distinguished two structurally different patterns: a geographically stable TB detection deficit in Ahoada West that persisted across four consecutive years despite dramatic increases in state-wide notification, and an episodic, single-year TB/HIV hotspot confined to the industrial corridor of Port Harcourt, Obio/Akpor, and Eleme that did not recur. These findings indicate that TB case-finding and HIV-testing integration operate through distinguishable geographic and programmatic pathways within the same state, and that resource allocation decisions should be informed by year-specific, LGA-resolution cluster testing rather than by pooled or purely

descriptive spatial comparison.

Recommendations

The confirmed Ahoada West Low-Low coldspot should be treated as a priority target for mobile diagnostic outreach, given its four-year statistical persistence despite state-wide programme expansion elsewhere. Because the Port Harcourt, Obio/Akpor, and Eleme corridor is the only zone in which a confirmed TB/HIV High-High cluster has been documented, HIV testing integration within TB services should be strengthened and monitored there specifically, to determine whether the 2022 surge reflected a sustainable service gain or a transient campaign effect. Given the magnitude of the adjusted working-age effect on co-infection, workplace-based screening should be extended to petroleum-sector facilities, construction sites, and market associations that concentrate this age group. Surveillance practice should also change in light of the pooled-analysis finding, with year-by-year rather than pooled spatial cluster testing adopted as routine, since this study demonstrates that pooled analysis would have misclassified a transient co-infection cluster as a stable hotspot. Finally, replication of the cluster analysis at ward or facility-catchment resolution, using a larger number of spatial units, would resolve whether the absence of a confirmed TB hotspot reflects a true absence of urban-core clustering or insufficient statistical power at LGA resolution.

Article Information

Funding: No external funding was received for this study.

Author Contributions: O.D. Ihekwaba: Conceptualization, Methodology, Data curation, Formal analysis, Writing – original draft, Writing – review & editing; A.I. Wegbom: Writing – review & editing, Supervision; C.K. Edet: Writing – review & editing.

Ethical Approval: Ethical approval was obtained from the Rivers State Ministry of Health and Hospital Management Board and from the Research Ethics Committee.

Conflict of Interest: The authors declare no conflict of interest.

Data Availability: Data available on reasonable request.

Disclaimer (Artificial Intelligence): The author(s) hereby declare that NO generative AI technologies such as Large Language Models (ChatGPT, COPILOT, etc).

References

[1] World Health Organization. *Global tuberculosis report 2024*. World Health Organization, Geneva, 2024.

[2] P. R. Murray, K. S. Rosenthal, and M. A. Pfaller. *Medical microbiology*. Elsevier, Philadelphia, 9th edition, 2021.

[3] B. R. Bloom, R. Atun, T. Cohen, C. Dye, H. Fraser, G. B. Gomez, G. Knight, M. Murray, E. Nardell, E. Rubin, J. Salomon, A. Vassall, G. Volchenkov, D. White, R.and Wilson, and P. Yadav. Tuberculosis. In K. K. Holmes, S. Bertozzi, B. R. Bloom, and P. Jha, editors, *Major infectious diseases*, pages 233–313. The World Bank, Washington (DC), 3rd edition, 2017.

[4] K. Wong, J. Nguyen, L. Blair, M. Banjanin, B. Grewal, S. Bowman, H. Boyd, G. Gerstner, H. J. Cho, D. Panfilov, C. K. Tam, D. Aguilar, and V. Venketaraman. Pathogenesis of human immunodeficiency virus-Mycobacterium tuberculosis co-infection. *Journal of clinical medicine*, 9(11):3575, 2020.

[5] P. M. Sharp and B. H. Hahn. Origins of HIV and the AIDS pandemic. *Cold Spring Harb Perspect Med*, 1(1):a006841, 2011.

[6] G. Pantaleo, C. Graziosi, and A. S. Fauci. The immunopathogenesis of human immunodeficiency virus infection. *The New England journal of medicine*, 328(5):327–335, 1993.

[7] A. Van't Hoog, K. Viney, O. Biermann, B. Yang, M. M. Leeflang, and M. W. Langendam. Symptom- and chest-radiography screening for active pulmonary tuberculosis in HIV-negative adults and adults with unknown HIV status. *The Cochrane database of systematic reviews*, 3(3):CD010890, 2022.

[8] M. Singer, N. Bulled, B. Ostrach, and E. Mendenhall. Syndemics and the biosocial conception of health. *Lancet*, 389(10072):941–950, 2017.

[9] C. K. Kwan and J. D. Ernst. HIV and tuberculosis: a deadly human syndemic. *Clinical microbiology reviews*, 24(2):351–376, 2011.

[10] E. E. Reward, A. C. Ike, S. O. Muo, B. F. Soga-Oke, and E. M. Mbaawuaga. Coinfection of tuberculosis and HIV in Nigeria: a systematic review and meta-analysis. *AIDS reviews*, 23(2), 2022.

[11] J. Obasanya, S. T. Abdurrahman, O. Oladimeji, L. Lawson, R. Dacombe, N. Chukwueme, T. Abiola, G. Mustapha, C. Sola, J. Dominguez, and L. E. Cuevas. Tuberculosis case detection in Nigeria: the unfinished agenda. *Tropical medicine & international health*, 20(10):1396–1402, 2015.

[12] F. E. Ejeh, A. Undiandeye, K. Okon, H. M. Kazeem, and A. C. Kudi. Isolation and immunological detection of Mycobacterium tuberculosis from HIV and non-HIV patients in Benue State, Nigeria. *Ethiop J Health Sci*, 30(1):55–64, 2020.

[13] I. O. Okonko, A. Anyanwu, A. Osadebe, and N. Odu. HIV and Tuberculosis Co-infection in a Highly HIV-infected Population of Rivers State, Nigeria. *Journal of Immunoassay and Immunochemistry*, 39(6):636–646, 2018.

[14] I. Des-Wosu, G. Owhonda, and C. I. Tobin-West. Spatial-temporal Distribution of Tuberculosis Infections in Rivers State from 2009-2018. *Journal of Epidemiological Society of Nigeria*, 4(2):7–12, 2021.

[15] S. A. Abdullahi, M. Smelyanskaya, S. John, H. I. Adamu, E. Ubochioma, I. Kennedy, F. A. Abubakar, H. A. Ago, R. Stevens, and J Creswell. Providing TB and HIV outreach services to internally displaced populations in northeast Nigeria: results of a controlled intervention study. *PLoS Med.*, 17(9):e1003218, 2020.

[16] C. Ogbudebe, D. Jeong, B. Odume, O. Chukwuogo, C. Dim, S. Useni, O. Okuzu, C. Malolan, D. Kim, F. Nwariaku, N. Nwokoye, S. Gande, D. Nongo, R. Eneogu, T. Odusote, S. Oyelaran, O. Chijioke-Akaniro, N. Nihalani, C. Anyaike, and M. Gidado. Identifying hot spots of tuberculosis in Nigeria using an early warning outbreak recognition system: retrospective analysis of implications for active case finding interventions. *JMIR public health and surveillance*, 9:e40311, 2023.

[17] C. F. McQuaid, A. Vassall, T. Cohen, K. Fiekert, and R. G. White. The impact of COVID-19 on TB: a review of the data. *The international journal of tuberculosis and lung disease*, 25(6):436–446, 2021.

[18] K. A. Levin. Study design VI. Ecological studies. *Evidence-based dentistry*, 7(4):108, 2006.

[19] Institute of Human Virology Nigeria. *HIV epidemiological profile for Rivers State*. IHVN, Abuja, 2025.

[20] National Agency for the Control of AIDS. *Nigeria HIV/AIDS indicator and impact survey:technical report*. NACA, Abuja, 2023.

[21] I. O. Okonko, I. U. Ejike, C. Innocent-Adiele, and T. I. Cookey. HIV coinfections with tuberculosis among HIV-1 infected individuals in old Cross River State, Nigeria. *Journal of Immunoassay and Immunochemistry*, 41(3):497–513, 2020.

[22] M. Okeke, P. M. Eze, A. E. Chukwudebelu, C. J. Nwankwo, N. K. Eze, U. U. Okafor, I. C. Abonyi, E. E. Okereke, K. O. Obasi, O. A. Ede, C. P. Ejikeugwu, C. I. Ilo, and J. O. Okafor. Tuberculosis and HIV/AIDS coinfection in patients attending Directly Observed Treatment Short-course (DOTS) centers in Anambra State, Nigeria: A retrospective study. *Health science reports*, 7(6):e2201, 2024.

[23] S. Bartholomew Ochonye, O. F. Sanni, G. Emmanuel, P. Umoh, A. Kalaiwo, R. Abang, P. Amechi, M. Ahkigbe, S. Akinpelumi, and O. Motilewa. A retrospective study of tuberculosis prevalence and associated factors among HIV-positive key populations in Nigeria. *PLOS global public health*, 4(7):e0003461, 2024.

[24] G. Aliyu, S. S. El-Kamary, A. Abimiku, W. Blattner, and M. Charurat. Demography and the dual epidemics of tuberculosis and HIV: analysis of cross-sectional data from sub-Saharan Africa. *PLOS ONE*, 13(9):e0191387, 2018.

[25] A. M. Oyefabi, C. I. Tobin West, S. Ameh, E. N. Jiya, A. Sadiq, H. Dauda, and M. Onoh. Predictors of mortality among drug-resistant tuberculosis patients in Kaduna State, Nigeria. *Nigerian journal of clinical practice*, 26(6):825–831, 2023.

[26] H. O. Nwoga, C. P. Igweagu, and G. C. Umeh. Prevalence and determinants of TB/HIV coinfection: the double tragedy of infectious disease burden. A 5-year retrospective study in a tertiary health facility in Enugu State, Nigeria. *BMJ Open*, 14(11):e088287, 2024.

[27] B. G. Link and J. C. Phelan. *Fundamental-cause theory*, pages 65–82. Springer Nature Switzerland, Cham, 2025.

[28] J. John and R. Z. Kompithra. Eco-epidemiology triad to explain infectious diseases. *The Indian journal of medical research*, 158(2): 107–112, 2023.

[29] M. Milaham, M. Van Gurp, O. J. Adewusi, O. C. Okonuga, H. Ormel, B. Tristan, S. Adejo, A. Yusuf, and M. Gidado. Assessment of tuberculosis case notification rate: spatial mapping of hotspot, coverage and diagnostics in Katsina State, north-western Nigeria. *Journal of public health in Africa*, 13(3):2040, 2022.

[30] N. Krieger. Ecosocial theory of disease distribution. In *Epidemiology and the people's health Theory and context*, pages 247–292. Oxford University Press, New York, 2024.

[31] E. Baffoe-Twum, E. Asa, B. Awuku, and A. Essegbey. Investigating the trends in traffic count data utilizing global and local spatial autocorrelation. *Journal of Statistics and Management Systems*, 29(1):1–37, 2025.

[32] R. Tao and Y. Chen. *Applying local indicators of spatial association to analyze longitudinal data: the absolute perspective*. Geographical Analysis, 2022. URL https://doi.org/10.1111/gean.12323.